PERGAMON

International Journal of Solids and Structures 40 (2003) 5097–5107

INTERNATIONAL JOURNAL OF SOLIDS and STRUCTURES

www.elsevier.com/locate/ijsolstr

Response suppression and transient behavior in a nonlinear active cochlear model with feed-forward

Kian-Meng Lim [a,*], Charles R. Steele [b]

[a] Department of Mechanical Engineering, National University of Singapore, 9 Engineering Drive 1, Singapore 117576, Singapore
[b] Department of Mechanical Engineering, Division of Mechanics and Computation, Stanford University, Stanford, CA 94305-4035, USA

Received 11 September 2002; received in revised form 4 January 2003

Abstract

A nonlinear active cochlear model is used to simulate the steady-state frequency response and transient response to clicks of the basilar membrane. The model includes the three-dimensional viscous fluid effects, an orthotropic cochlear partition with dimensional and material property variation along its length, and a nonlinear active feed-forward mechanism to represent the activity of the outer hair cells. A hybrid asymptotic and numerical method is used to provide a fast and efficient iterative procedure for modeling and simulation of the nonlinear responses in the active cochlea. The simulation results exhibit some of the characteristic nonlinear behavior of the basilar membrane commonly observed in experimental measurements, such as significant amplification and sustained "ringing" in the transient response at low stimulus level. The simple feed-forward mechanism is able to capture the properties of the noncausal active process in the cochlea without a second filter or resonance.

Keywords: Active cochlear model; Feed-forward; Nonlinear suppression; Transient response

1. Introduction

Experimental measurements on frequency response of the basilar membrane (BM) in the basal turn of the mammalian cochlea often show a sharp tuning at the characteristic frequency (CF) of that location (Rhode, 1971; Sellick et al., 1982). Kim et al. (1980) postulated that there is a "local activity" that amplifies the motion of the BM in this region of sharp tuning. Recently, it is believed that this activity that enhances the cochlea's sensitivity and frequency selectivity can be attributed to the electromotility of outer hair cells (OHC) in the organ of Corti (Ashmore, 1987). It also accounts for the nonlinear behavior in the basilar membrane responses measured in the live cochlea (Ruggero et al., 1997; Recio et al., 1998) resulting from the saturation in the force exerted by the OHCs.

* Corresponding author. Tel.: +65-6874-8860; fax: +65-6779-1459.
E-mail address: limkm@nus.edu.sg (K.-M. Lim).

0020-7683/$ - see front matter © 2003 Elsevier Ltd. All rights reserved.
doi:10.1016/S0020-7683(03)00257-9

In this paper, we incorporate this nonlinear activity of the OHCs into a three dimensional cochlear model with two fluid scale and a flexible partition. The active OHCs are modeled with a feed-forward mechanism (Steele et al., 1993; Geisler and Sang, 1995; Steele and Lim, 1999) that accounts for their longitudinal tilt, so that the OHCs push on the BM slightly downstream of the sensing location of their stereocilia. We use this model to investigate if such a simple mechanism can capture the gross characteristic behavior in an active cochlea. The model is used to simulate the BM responses due to the tone and click inputs of various stimulus levels at the stapes and these results are compared with experimental measurements from Ruggero et al. (1997) and Recio et al. (1998).

2. Formulation

The present nonlinear model (Fig. 1) is based on a macroscopic three-dimensional model consisting of a slender fluid chamber with rigid walls divided longitudinally by a cochlear partition that includes the flexible BM. The viscous fluid effects and the variation of dimensions and orthotropy of the BM are included. Prescribed displacement of the stapes sets the fluid into motion resulting in traveling waves on the BM. Due to the variation in the BM stiffness, each location along the length vibrates with different amplitude for various input frequencies. At a particular location, the frequency that gives the largest amplitude is known as the CF for that location. The vibration of the BM in the live cochlea is actually amplified by the motility of the OHCs which exert an additional force on the BM. This activity of the OHC is modeled using a nonlinear feed-forward mechanism as depicted in Fig. 2. The OHC senses the motion of the BM via the force acting on the cilia F_{cilia} that is transmitted by the arches of Corti. This shearing force on the cilia triggers an electro-chemical process of ions flow, causing the OHC to push back on the BM with a force F_{cell}. Due to the longitudinal tilt of the OHC, this force is applied on a location downstream of the sensing cilia location, separated by a distance Δ. The detailed formulation for the model is given in Lim and Steele

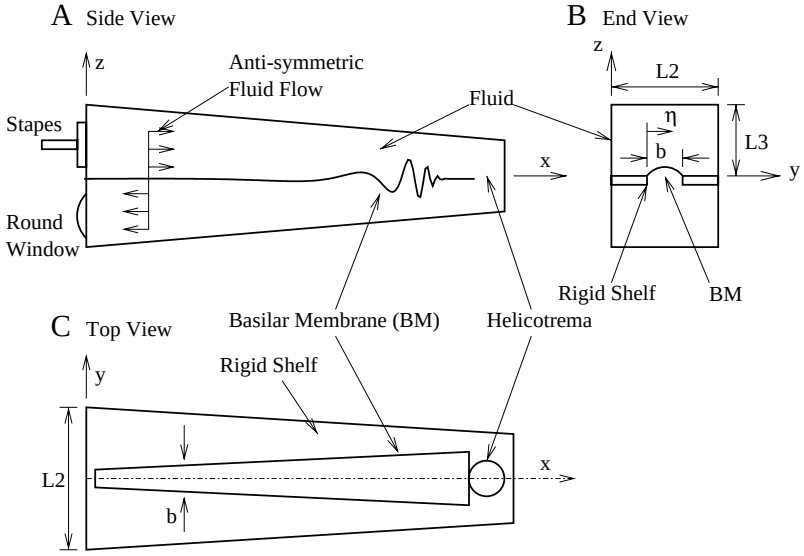

Fig. 1. Schematic drawing of the cochlear model. The side and end views are shown in A and B respectively. The top view of the cochlear partition is shown in C. A typical basilar membrane response due to a harmonic excitation is shown.

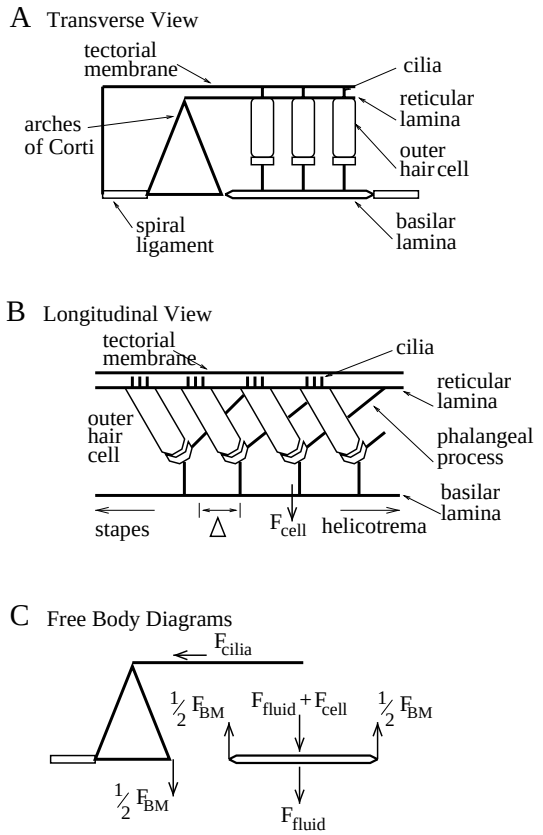

Fig. 2. Feed-forward mechanism of the outer hair cells. Transverse view A and the longitudinal view B are shown. Free body diagrams in C show the balance of forces on the BM and arches.

(2002). Here, a brief outline of the formulation is presented with focus on the iterative solution used to deal with the nonlinear activity in the model.

In the present three-dimensional model, the fluid displacement $\vec{u}$ and pressure p_f fields in the chamber are represented in terms of a scalar potential ϕ and a vector quantity $\vec{\psi}$

$$\vec{u} = \nabla\phi + \nabla \times \vec{\psi} \tag{1}$$

$$p_f = -\rho_f \ddot{\phi} \tag{2}$$

where ρ_f is the density of the fluid, ∇ is the gradient operator in space and the dot ($\dot{}$) represents the derivative in time. The quantities ϕ and $\vec{\psi}$ are formulated in the frequency domain, assuming that a harmonic excitation with frequency ω is being applied at the stapes. They are also assumed to have the following forms to enforce the boundary conditions of no outward fluid flow at the three rigid walls of the chamber:

$$\phi(x,y,z,t) = e^{-i\omega t}\Phi(x)\sum_m R_m(x)\cos\left(\frac{m\pi y}{L_2}\right)\cosh\left(\beta_m(x)(L_3 - z)\right) \tag{3}$$

$$\vec{\psi}(x,y,z,t) = \begin{pmatrix} \psi^1 \\ \psi^2 \\ \psi^3 \end{pmatrix} = \mathrm{e}^{-\mathrm{i}\omega t} \sum_m \mathrm{e}^{\gamma_m(x) z} \begin{pmatrix} \Psi^1_m(x) \sin\left(\dfrac{m\pi y}{L_2}\right) \\ \Psi^2_m(x) \cos\left(\dfrac{m\pi y}{L_2}\right) \\ 0 \end{pmatrix}. \tag{4}$$

The coefficients Ψ^1_m and Ψ^2_m are related to the amplitude Φ and R_m through no-slip boundary conditions on the cochlear partition where the tangential displacements are zero. The coefficients R_m are determined by matching the normal displacement of the fluid with the displacement profile of the partition.

The displacement profile of the cochlear partition w is assumed to take the following form

$$w(x,\eta,t) = \mathrm{e}^{-\mathrm{i}\omega t} \mathscr{W}(x) \sin\frac{\pi\eta}{b} \tag{5}$$

where b is the width of the pectinate zone and $\mathscr{W}$ is the amplitude of displacement. The pectinate zone is modeled as an orthotropic plate whose bending motion is governed by the following equation:

$$\rho_{\mathrm{p}} h \ddot{w} + \frac{\partial^2}{\partial x^2}\left(D_{11}\frac{\partial^2 w}{\partial x^2}\right) + 2\frac{\partial^2}{\partial x \partial y}\left(D_{12}\frac{\partial^2 w}{\partial x \partial y}\right) + \frac{\partial^2}{\partial y^2}\left(D_{22}\frac{\partial^2 w}{\partial y^2}\right) = p_{\mathrm{p}} \tag{6}$$

where h and ρ_{p} are the thickness and density of the pectinate zone respectively, p_{p} is the pressure acting on it, and D_{11}, D_{12}, and D_{22} are the bending stiffness components which take into account the fiber density and sandwiched nature of the BM.

The active OHCs exert a force on the BM to amplify its motion. Due to the longitudinal tilt of the OHCs, a feed-forward mechanism is used in this model. Here, the force F_{c} exerted by the OHC at the location $x + \Delta$ on the BM is assumed to be proportional to the total force F_{BM} acting on the BM at the location x

$$F_{\mathrm{c}}(x+\Delta,t) = \alpha(x,t) F_{\mathrm{BM}}(x,t) \tag{7}$$

$$= \alpha(x,t)(2F_{\mathrm{f}}(x,t) + F_{\mathrm{c}}(x,t)) \tag{8}$$

where $\alpha(x,t)$ is the feed-forward gain. The total force acting on the BM is in turn given by the sum of forces from the two fluid chambers F_{f} and the OHCs. The longitudinal distance Δ between the sensing cilia location and the supporting Dieter's cell location of an OHC may be determined from anatomical data. It is a critical parameter in the feed-forward mechanism as it accounts for the phase lead of the OHC force over the fluid force acting on the same cross-section of the BM. In the region whose CF is close to the excitation frequency, this phase difference in the OHC force results in a net input of energy over each time cycle giving a significant amplification of the BM motion. If the longitudinal tilt of the OHC is ignored and the feed-forward distance reduced to zero, the amplification effect of the feed-forward mechanism will diminish because the OHC force will now act in phase with the fluid forces. In this case, the OHC force effectively increases the fluid forces acting on the BM by a small factor of $\alpha/(1-\alpha)$ (typically $\alpha < 0.5$) which would not give any large amplification.

The force from the OHC is known to saturate with the motion of the BM as shown in Fig. 3. From the relation in Eq. (8), the gain factor α is thus given by the chord joining a point on the curve to the origin. This gain factor remains fairly constant for small basilar membrane displacement and decreases to a small value as the basilar membrane displacement increases due to this saturation in the outer hair cell force.

To solve for the BM response, the fluid and partition displacements are matched at their interface so that $\mathscr{W}(x) = \Phi(x)$. Next, the requirement of force balance on the partition leads to the following eiconal equation:

$$K_{\mathrm{p}}(n) - 2\left(1 + \frac{\alpha}{\mathrm{e}^{\mathrm{i}n\Delta} - \alpha}\right)\rho_{\mathrm{f}}\omega^2 h_{\mathrm{f}}(n) = 0 \tag{9}$$

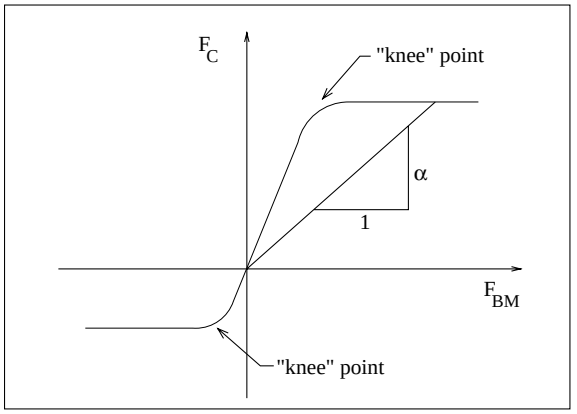

Fig. 3. Profile of the outer hair cell force F_c showing the saturation with the force acting on the basilar membrane F_{BM}. The feed-forward gain factor α is given by the gradient of the chord joining a point on the graph to the origin.

where K_p is the effective stiffness of the pectinate zone, h_f is the effective thickness of fluid that contributes to the mass in the system. These quantities depend on the local wavenumber $n(x)$ which is approximated by $n^2 \approx -\phi_{,xx}/\phi$. The term $\alpha/(e^{in\Delta} - \alpha)$ accounts for the active force from the OHCs. Finally, by imposing the continuity condition for each cross-section of the fluid duct, we obtain the following transport equation:

$$\frac{d^2}{dx^2}\left(\frac{\mathscr{W} R_0 \sinh nL_3}{n}\right) + \mathscr{W} R_0 n \sinh nL_3 = 0 \tag{10}$$

for a fluid duct with constant width and height. An equation of the similar form can also be derived for a fluid duct with varying cross-sectional area (Lim, 2000).

To find the response of the partition due to a harmonic excitation at the stapes, we first solve for the wavenumber $n(x)$ using the eiconal equation (9). Subsequently, these wavenumbers are substituted into the transport equation (10) and this differential equation is solved to obtain the response amplitude $\mathscr{W}$. The boundary conditions imposed are the displacement input at the stapes and zero pressure at the helicotrema. The transport equation is solved using a combination of the asymptotic (WKB) method in the short wave region (where n is large) and numerical Runge–Kutta method in the long wave region (where n is small). In fact, these two methods complement each other very well as they provide a fast and accurate answer in the region where the other would fail to do so.

This hybrid WKB-numeric solution provides a fast and efficient computation that is essential for the iterative solution needed for a nonlinear problem. The nonlinearity is manifested in the dependence of the gain factor α on the amplitude of the response $\mathscr{W}$ due to the saturation of OHC force. In the solution process, an initial guess of the feed-forward gain $\alpha(x)$ at each grid point is made based on the amplitude (approximated by the WKB method) of the response at the grid point that is immediately upstream. Once the first set of wavenumbers $n(x)$ and BM response $\mathscr{W}(x)$ are determined, subsequent iterations on the solution are obtained using either the relaxation method or secant method. The iteration process stops when the relative error between successive values of the feed-forward gain α falls within a certain tolerance (1% is used in the present case) and a converged solution for the response is obtained. This iteration process is illustrated in Fig. 4.

Although the present formulation is based in the frequency domain where the excitation from the stapes is harmonic, the model can be extended to provide the transient response of the BM subjected to a click input at the stapes. This is done by first applying a Fourier transform on the stapes input to obtain its harmonic components. Each harmonic component is then analyzed using the above formulation in the

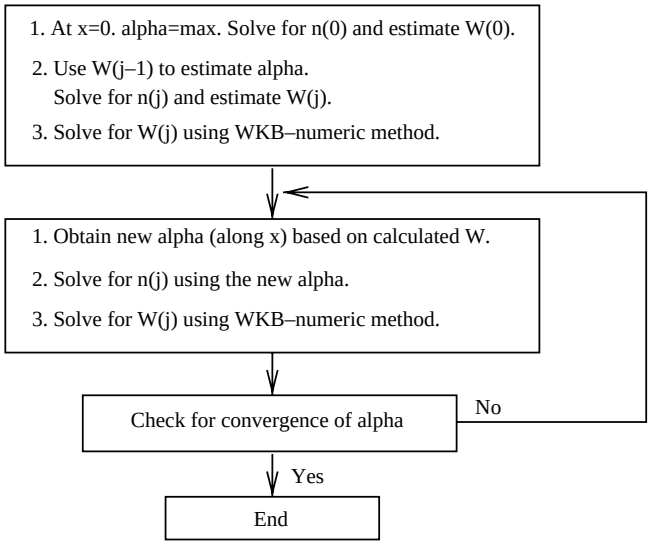

Fig. 4. Flowchart illustrating the iterative solution process of obtaining the wavenumber and BM response.

frequency domain. Finally, the synthesis of these harmonic responses using the inverse Fourier transform gives the transient response of the BM. In the present case, each harmonic analysis is performed independently so that the various frequency components are not coupled to each other. This is similar to the quasilinear analysis conducted by Kanis and de Boer (1993). The validity of such an approach will need to be verified by a model that include the cross-coupling among frequency components or a model formulated in the time domain. Development of such a model will be pursued in the future.

3. Results

The above model is used to simulate the BM responses to tones and clicks presented at the stapes. The input parameters to the model are based on the anatomy of the chinchilla cochlea used by Lim and Steele (2002). The parameters that are difficult to quantify are the "knee" points in the OHC force saturation curve in Fig. 3, and these are probably dependent on the complex micro-mechanics of the organ of Corti and the mechanoelectrical transduction process of the OHC. However, the absolute values of these quantities are not important for obtaining relative response of the BM to the stapes input. These points of saturation just provide a reference for a relative measure for the level of high or low stimulus at the stapes. For the present calculation, the set of "knee" values is calibrated against experimental measurements in the chinchilla by Ruggero et al. (1997) so that the calculated results are in a comparable region of the stimulus level as used in the experiments. The stapes input to the model is varied from low to high over a range corresponding to 0–90 dB SPL in the experiments. Over this range, the OHC force crosses over the "knee" region, from being proportional to the BM force to being saturated in value. The maximum gain factor used here is $\alpha = 0.2$.

3.1. Frequency response

The BM response when the stapes is excited at a frequency of 10 kHz at various input levels (20–80 dB SPL) is shown in the top panel of Fig. 5. The plot gives the BM amplitude normalized by the stapes input

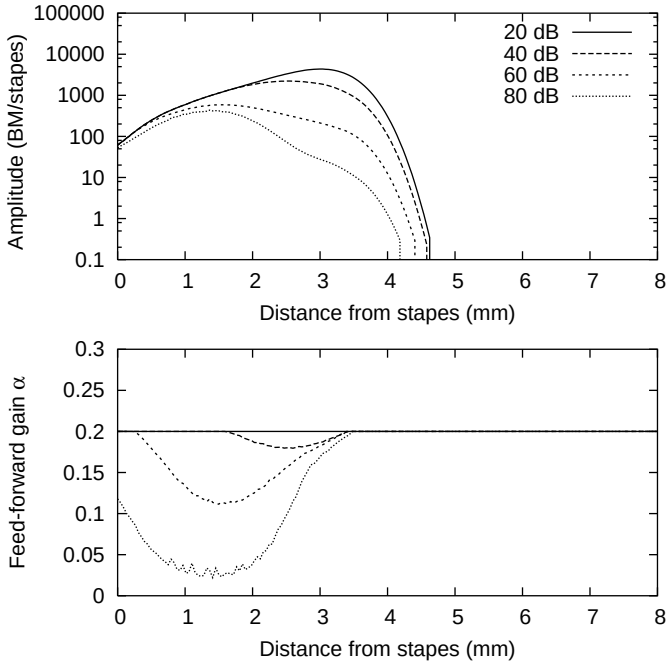

Fig. 5. The top panel shows the amplitude of the steady state response of BM normalized to the stapes input when excited at 10 kHz for various levels of stimulus input. The lower panel shows the feed-forward gain factor along the basilar membrane for various levels of stimulus input.

against the distance along the cochlear duct measured from the stapes. For a low stimulus level (20 dB SPL), the amplitude is maximum at a location 3 mm from the stapes. Thus, this location has a CF of 10 kHz. However, for higher stimulus level, the peak of the response is shifted basally towards the stapes. The normalized amplitude of the BM response also decreases indicating the suppression of activity with high stimulus level. This is evident from the lower panel of Fig. 5 which shows the feed-forward gain factor α variation along the length of the cochlea for the various stimulus level. For high stimulus level of 80 dB SPL, the gain factor is reduced to near zero where the peak of the response amplitude occurs. As the stimulus level is reduced, the gain factor is progressively restored to the maximum value of 0.2.

The BM velocity at the location 3 mm from the stapes is plotted against the the input level in Fig. 6. It shows a linear increase for low input level up to about 30 dB SPL, but turns nonlinear as the activity in the OHC get suppressed with higher stimulus level. At high input level, the response is suppressed by about 30–40 dB. This nonlinear suppression in response with stimulus level is also observed in experimental measurements by Ruggero et al. (1997), as shown by the points in the plot.

The frequency response of the same location (3 mm from the stapes) over a range of excitation frequencies is shown in Fig. 7. The stimulus level is varied from 20 to 80 dB SPL. Each curve gives the amplitude and phase of the response on the basilar membrane normalized by the stapes input displacement. For a low input level, a large amplification is present due to the active process in the cochlea. With increasing stimulus level, the response is suppressed and the CF is shifted down to about 6 kHz. These essential gross features of the response are typically observed in experimental measurements such as those of Ruggero et al. (1997) which are given by the points in the plot. The experimental results are indifferent to the input level up to about 7 kHz (results for 20 dB SPL plotted with dark squares overlap with the results for 80 dB SPL plotted with open squares). This phenomenon also shows up in the simulation results up to

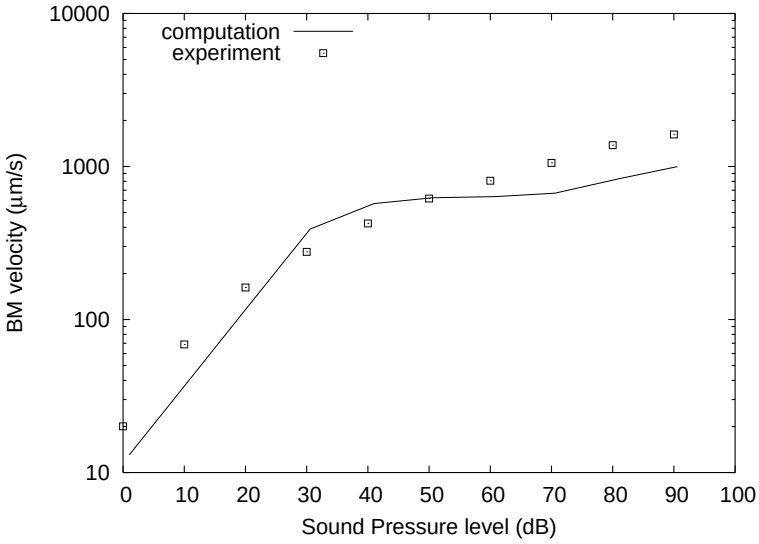

Fig. 6. Nonlinear compression of the BM response at $x = 3$ mm with stimulus level. The BM velocity linear increase with stimulus level is suppressed, or compressed nonlinearly, as the stimulus level increases. Experimental measurements (indicated as points in the plot) by Ruggero et al. (1997) are included for comparison.

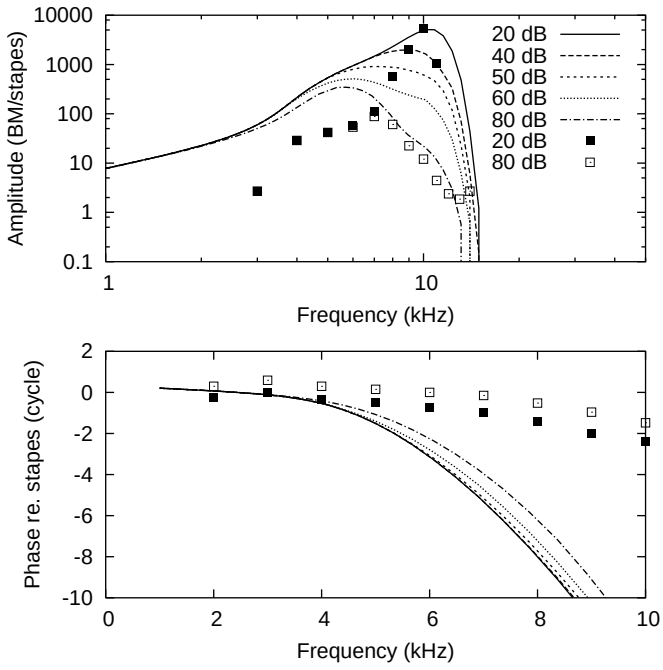

Fig. 7. Frequency response of BM at $x = 3$ mm normalized to the stapes input for various level of stimulus input from 20 to 80 dB SPL. The amplitude plot (top panel) is given on a log scale and the phase plot (lower panel) is given on a linear scale. The simulation results are given by lines in the plots. Experimental measurements (indicated as points in the plots) by Ruggero et al. (1997) are included for comparison.

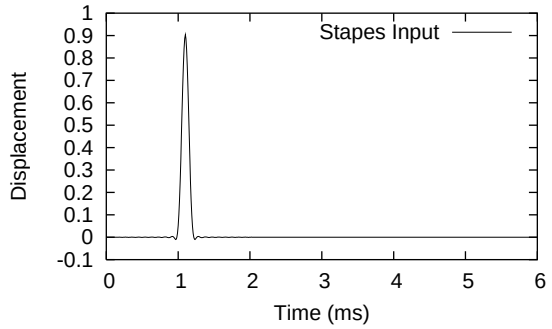

Fig. 8. Normalized profile of click input at the stapes for transient response simulation. The actual displacement input is scaled accordingly for the low and high stimulus levels.

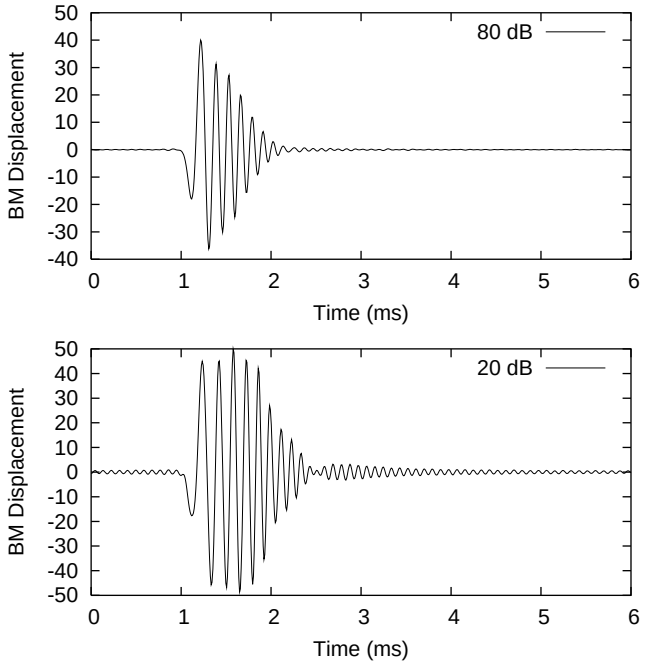

Fig. 9. Normalized BM response at $x = 2$ mm (CF = 15 kHz) to click input. For low stimulus level of 20 dB SPL (lower panel), the response shows a longer "ringing" that for high stimulus level of 80 dB SPL (upper panel).

about 5 kHz. The response amplitude rolls off rapidly beyond 10 kHz as depicted by the simulation results, and this is also commonly observed in experimental measurements. For the phase of the BM response relative to the stapes motion, the simulation results show a larger accumulation in phase than the experimental results. This discrepancy could probably be due to the assumption that the stapes in the model is located at the end of the fluid duct ($x = 0$) whereas the actual position of the stapes in the cochlea extends over a small portion of the basal end of the BM. There is also a possibility that the current simplistic feedforward mechanism has missed out on other essential mechanics or processes present in the cochlea. Despite such differences, the phase of the responses calculated from the model behaves in a similar manner

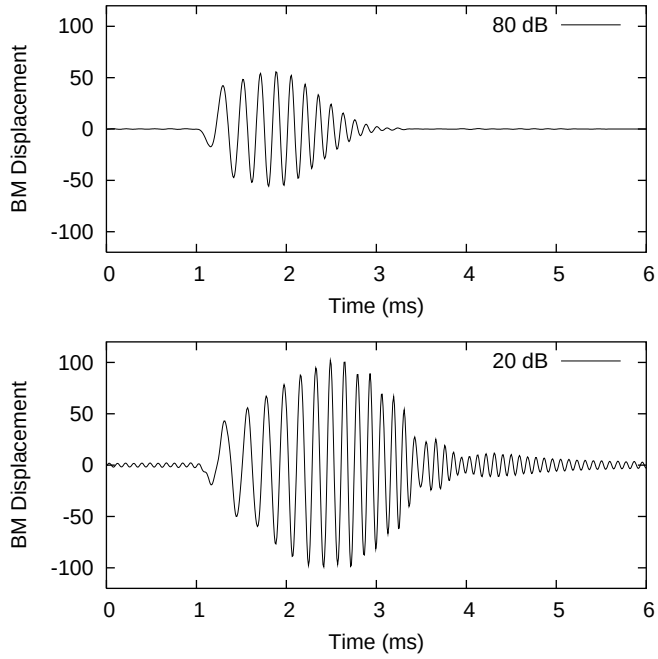

Fig. 10. Normalized BM response at $x = 3$ mm (CF = 10 kHz) to click input. For low stimulus level of 20 dB SPL (lower panel), the response shows a longer "ringing" that for high stimulus level of 80 dB SPL (upper panel).

as the experimental results in their indifference to the stimulus level, i.e. the phases do not change much with the stimulus level. This is also an indication of the invariance of fine time structure to stimulus intensity (Shera, 2001).

3.2. Transient response

A series of clicks with a time profile as shown in Fig. 8 are repeatedly applied at the stapes at a time interval of 10 ms. Figs. 9 and 10 show the transient response of the BM at points 2 and 3 mm from the stapes respectively. These responses are again normalized by the stapes displacement which are applied in turn at 20 and 80 dB SPL. Similar to the frequency response, the normalized BM transient responses show a higher amplification at the low stimulus level. The nonlinear behavior of the BM is also reflected by the differences in the shape of the transient responses. For low stimulus level, there is usually a second lobe at the tail of the transient response after the main envelope decreases to zero. At low stimulus level, a sustained "ringing" effect in the BM response is also obtained, i.e. the BM displacement takes a longer time to settle back to zero. At high stimulus level, the "ringing" effect is reduced as the OHC force saturates, and the feed-forward gain factor α decreases. This phenomenon is also observed in experiments by Recio et al. (1998) where the BM response in the live cochlea exhibits more "ringing" when stimulated by a low stimulus level of clicks as compared to a high stimulus level.

4. Concluding remarks

An active cochlear model has been constructed to include a nonlinear feed-forward mechanism to represent the OHCs in the organ of Corti. This model is used to simulate the BM steady-state frequency

response to tones and transient response to clicks presented at the stapes. The simulation results is able to capture the gross characteristic nonlinear behavior of the BM commonly observed in experimental measurements. These include significant frequency response suppression and decrease in CF with high stimulus level, invariance of phase with stimulus level, and prolong "ringing" in the transient response to clicks for low stimulus level.

However, there are some differences between the simulation results and experimental measurements. Besides mismatch in some of the details in the responses, the large difference in the phase accumulation of the frequency response may indicate that the current model may be too simple to capture all the right mechanics in the cochlea. One deficiency in the present model is probably the lack of a feedback mechanism commonly used in several other active cochlear models (Neely, 1985; Geisler, 1991). In fact, de Boer and Nuttall (2002) pointed out that the active process in the cochlea would contain a combination of both feed-forward and feedback based on their analysis of experimental results of the BM response. Nevertheless, the present feed-forward mechanism addresses the findings of de Boer and Nuttall (2002) on the two basic properties of the active process: (i) the active process is noncausal, and (ii) the active process results from spatial interaction without any filtering or resonance. For the first property, it is noted that the feed-forward mechanism actually pushes on a location on the BM before the traveling wave reaches that location. The action applied is based on the future response of that location of the BM, and hence the mechanism is noncausal. The present model assumes that the OHC exerts a force immediately on the BM when it senses a shearing motion at its stereocilia. This is in agreement with the second property that no additional filtering or resonance is involved in the active process.

References

Ashmore, J.F., 1987. A fast motile response in the guinea-pig outer hair cells: The cellular basis of the cochlear amplifier. J. Physiol. 388, 323–347.

de Boer, E., Nuttall, A.L., 2002. Properties of amplifying elements in the cochlea. In: Biophysics of the Cochlea: From Molecules to Model. World Scientific, Singapore, pp. 228–236.

Geisler, C.D., 1991. A cochlear model using feedback from motile outer hair cells. Hearing Res. 54, 105–117.

Geisler, C.D., Sang, C., 1995. A cochlear model using feed-forward outer-hair-cell forces. Hearing Res. 95, 132–146.

Kanis, L.J., de Boer, E., 1993. Self-suppression in a locally active nonlinear model of the cochlea: a quasilinear approach. J. Acoust. Soc. Am. 94, 3199–3206.

Kim, D.O., Neely, S.T., Molnar, C.E., Matthews, J.W., 1980. A active cochlear model with negative damping in the partition: comparison with Rhode's ante- and post-mortem observations. In: Psychophysical, Physiological and Behavioural Studies in Hearing. Delft University Press, Delft, pp. 7–14.

Lim, K.M., 2000. Physical and mathematical cochlear models. Ph.D. Thesis, Stanford University.

Lim, K.M., Steele, C.R., 2002. A three-dimensional nonlinear active cochlear model analyzed by the WKB-numeric method. Hearing Res. 170, 190–205.

Neely, S.T., 1985. Mathematical modeling of cochlear mechanics. J. Acoust. Soc. Am. 78, 345–352.

Recio, A., Rich, N.C., Narayan, S.S., Ruggero, M.A., 1998. Basilar-membrane responses to clicks at the base of the chinchilla cochlea. J. Acoust. Soc. Am. 103, 1972–1989.

Rhode, W.S., 1971. Observations of the vibration of the basilar membrane in squirrel monkeys using the Mössbauer technique. J. Acoust. Soc. Am. 49, 1218–1231.

Ruggero, M.A., Rich, N.C., Recio, A., Narayan, S.S., Robles, L., 1997. Basilar-membrane responses to tones at the base of the chinchilla cochlea. J. Acoust. Soc. Am. 101, 2151–2163.

Sellick, P.M., Patuzzi, R., Johnstone, B.M., 1982. Measurement of basilar membrane motion in the guinea pig using the Mössbauer technique. J. Acoust. Soc. Am. 72, 131–141.

Shera, C.A., 2001. Intensity–invariance of fine time structure in basilar-membrane click responses: implications for cochlear mechanics. J. Acoust. Soc. Am. 110, 332–348.

Steele, C.R., Baker, G., Tolomeo, J., Zetes, D., 1993. Electro-mechanical models of the outer hair cell. In: Proc. Intl. Sym. Biophysics of Hair Cell Sensory Systems. World Scientific, Singapore, pp. 207–215.

Steele, C.R., Lim, K.M., 1999. Cochlear model with three-dimensional fluid, inner sulcus and feed-forward mechanism. Audiol. Neuro-Otol. 4, 197–203.